A Diagnostic Evaluation of Rainfall Predictability for Tropical Storm Agnes, June 1972

FREDERICK H. CARR AND LANCE F. BOSART

Department of Atmospheric Science, State University of New York at Albany, Albany, N.Y. 12222

(Manuscript received 1 November 1977, in final form 20 December 1977)

ABSTRACT

The problem of rainfall prediction for a tropical storm over the United States is examined from a diagnostic point of view. A moisture budget is constructed and the differences between the computed and observed precipitation are discussed. Although the areal averages were comparable, the point-by-point agreement was only fair. Stable and convective precipitation are then computed using methods common to many numerical models. The discrepancies between forecast and observed precipitation is assumed to be due to the incomplete formulation of the amount of moisture available for convection. This leads to an expression for the subgrid-scale moisture supply that provides the missing precipitation. Methods are then suggested in which the deficiencies of a parameterization scheme could be corrected during its use in a prognostic model.

1. Introduction

The accurate prediction of hurricanes or tropical storms remains a critical problem in the coastal areas of the United States. Three crucial aspects are the forecasts of 1) the storm intensity, 2) the location of storm landfall and its subsequent track, and 3) the spatial and temporal distribution and intensity of rainfall. Since most tropical storm damage arises from excessive rainfall and the resulting flooding, the third problem above is just as, if not more, important than the first two. It should be noted, of course, that these problems are not mutually exclusive; progress in one area should lead to concurrent improvement of the other forecast problems. Heavy rainfall events due to tropical systems can also extend well inland from coastal regions; notable examples are Camille in 1969, Celia in 1970, Agnes in 1972 and Eloise in 1975. In addition, as shown by Bosart and Carr (1978) for Tropical Storm Agnes, the influence of the cyclone may extend beyond its immediate periphery due to, for example, the additional northward moisture flux present on the eastern flank of the storm and its subsequent, possibly destructive, enhancement of an otherwise innocuous rain-producing situation.

Although many improvements in operational weather forecasting have been made over the last 15 years, quantitative precipitation forecasting has not yet been a beneficiary of this progress (Fawcett, 1977). Two primary reasons for the low level of skill are 1) the errors in the synoptic-scale mass fields predicted by the numerical models, and 2) the small space and time scales of many precipitation events, especially during summer. Since these convective and mesoscale features are too small to be resolved in a synoptic-scale forecast model, their collective effect on the large-scale fields has to be parameterized in the model. Although much research on parameterization techniques has also been carried out over the past 15 years, no definitive procedure has yet evolved.

In this study, we diagnostically compute stable and convective precipitation for Tropical Storm Agnes during its transit over the southeastern United States in June 1972. These values are compared with the observed rainfall amounts and the discrepancies are examined. The results will illustrate that even a diagnostic attempt to reproduce observed rainfall patterns is not a trivial problem. By assuming that the main source of error is due to the inadequacy of the convective parameterization scheme we derive some relationships that suggest methods by which the deficiencies of the scheme can be corrected during its application in a prognostic model.

Before we get to this last subject, however, the large-scale moisture budget for Agnes is examined for two time periods. Here the relationship between integrated moisture convergence and precipitation is examined in the context of both areal averages and individual grid points. The distribution of convective instability over the region is also compared to the observed rainfall patterns.

2. Moisture budget

Moisture budget or water vapor transport studies have been performed by many investigators since the

0027-0644/78/0363-0374$06.00

early 1950's (e.g., Spar, 1953; Benton and Estoque, 1954; Starr and White, 1955; Bradbury, 1957). In the work of Spar, Bradbury and others, the use of the computed moisture flux for quantitative precipitation forecasting was suggested. Although other methods were ultimately used for computing rainfall in numerical models, moisture budget studies continued to be used to evaluate the relationship between moisture convergence and rainfall on synoptic, meso and convective scales (Danard, 1968; Fankhauser, 1965; Hudson, 1971; Fernandez-Partagas and Estoque, 1974; Fritsch *et al.*, 1976). Hence, as a first step in examining the predictability of Agnes rainfall and its relation to moisture convergence, a simple moisture budget is performed for two time periods while Agnes is over the southeastern United States.

At each grid point, the moisture budget can be evaluated from

$$\frac{1}{g}\int_{p_t}^{p_s}\frac{\partial q}{\partial t}dp=-\frac{1}{g}\int_{p_t}^{p_s}\nabla\cdot q\mathbf{V}dp-\frac{1}{g}\int_{p_t}^{p_s}\frac{\partial q\omega}{\partial p}dp+E-P, \tag{1}$$

where p_s is surface pressure, p_t the top pressure level, E evaporation and P precipitation, and the remaining symbols have their usual meteorological meaning (see Appendix A for a list of symbols). The transport and storage of liquid and solid water are neglected in (1). For the purposes of this study evaporation is also neglected. If we assume that the vertical motion is zero at the earth's surface as well as at $p_t=100$ mb, then the second term on the right side of (1) vanishes and we may write

$$P=-\frac{1}{g}\int_{p_t}^{p_s}\frac{\partial q}{\partial t}dp-\frac{1}{g}\int_{p_t}^{p_s}\nabla\cdot q\mathbf{V}dp. \tag{2}$$

Wind, temperature and moisture data subjectively analyzed every 100 mb were used to evaluate the right side of (2). The computed divergences were modified according to O'Brien (1970) so that the integrated divergence sums to zero. The tendency term is estimated by a forward (backward) difference over 12 h for the first (second) time period. The computational domain over the eastern United States is divided into a 1° latitude-longitude grid. The observed hourly rainfall data, which were presented in detail in Bosart and Carr (1978), are used to compute 3 h totals centered around the radiosonde release times. These values are tabulated every 0.5° latitude-longitude and then averaged to obtain the required 1° mesh values.

Two consecutive time periods are examined: 1200 GMT 20 June and 0000 GMT 21 June 1972. During this time, Agnes moved northeast from south-central Georgia to the Georgia-South Carolina border. Concurrently a major rainfall event began around Wellsville, N.Y., which was separate from the Agnes rainshield. [See Bosart and Carr (1978) for a study of the evolution of this rainstorm as well as for maps of height, temperature, vorticity, vertical motion and moisture flux for this time period.] The results for the 1200 GMT period are shown in Figs. 1 and 2. Note that the observed rainfall rate chart (Fig. 1) does not include amounts over the oceans or west of

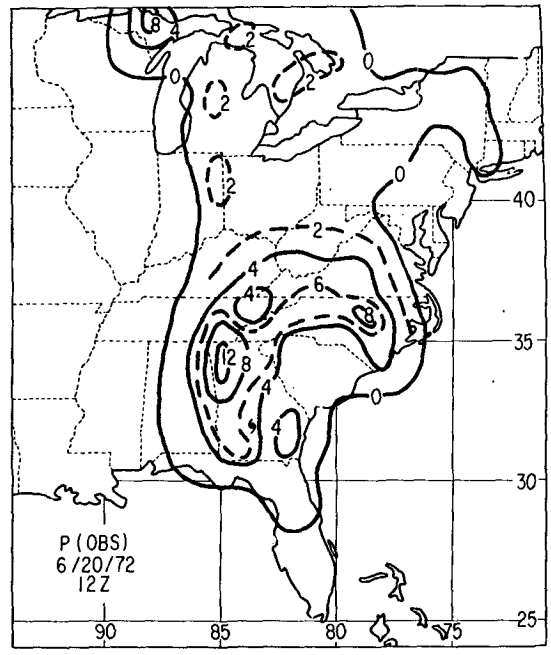

FIG. 1. Observed precipitation rate (10^{-4} kg s^{-1} m^{-2}) averaged over a 3 h period for 1200 GMT 20 June 1972. Conventional symbol denotes position of Agnes in this figure and hereafter.

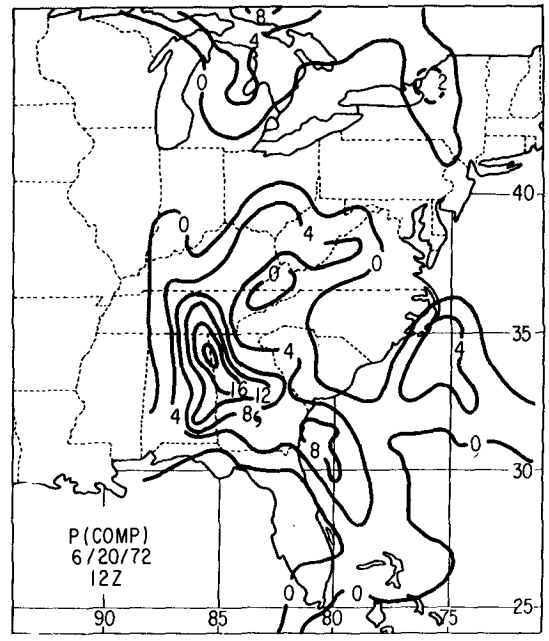

FIG. 2. Computed precipitation rate (10^{-4} kg s^{-1} m^{-2}) from the moisture budget for 1200 GMT 20 June 1972.

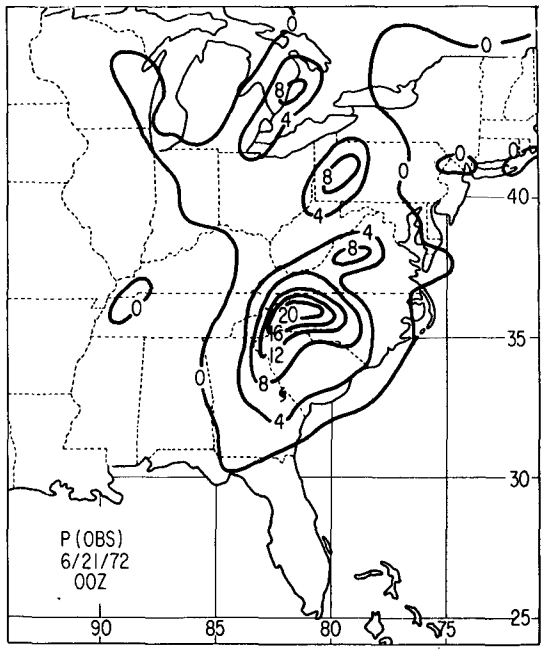

FIG. 3. Observed precipitation rate (10^{-4} kg s^{-1} m^{-2}) averaged over a 3 h period for 0000 GMT 21 June 1972.

the Mississippi River, Illinois and Wisconsin. The agreement with the computed precipitation rate (Fig. 2) ranges from poor to good. The rainfall rate maximum over northwest Georgia and the generally heavy rates over the southern Appalachians are predicted by (2). The observed rainfall rate in eastern North Carolina is not computed at all since the wind data indicated deep tropospheric divergence over that region. Agreement is only fair in the Great Lakes region.

At 0000 GMT the computed precipitation rate (Fig. 4) from (2) behaves even worse as a predictor of rainfall (Fig. 3). The observed heavy rainfall rate from Georgia to Virginia is separated by a near-zero area in western North Carolina. Agreement is good in eastern Michigan but not northeast of Lake Huron. It should be noted that, on the average, the horizontal moisture convergence term in (2) is five times larger than the tendency term. Thus Figs. 2 and 4 are indicating the predictive value of the vertical integral of horizontal moisture flux.

Although it was somewhat disturbing to find such large discrepancies, most of which are due to our lack of knowledge of the "true" divergence fields, we found, upon careful rechecking of the data, no justifiable reason for ignoring or changing any of the existing wind reports. Another small source of error [other than those made in deriving and finite differencing (2)] is the time lag involved between synoptic-scale moisture convergence and subsequent rainfall; this has been documented by Bradbury (1957), Fernandez-Partagas and Estoque (1974) among others.

An areal average approach to the evaluation of the moisture budget yields more encouraging results. For example, at 1200 GMT the mean observed precipitation for a 12°×12° box centered around Agnes (excluding ocean points) was 2.79×10^{-4} kg s^{-1} m^{-2} while the amount computed from (2) was 3.37×10^{-4} kg s^{-1} m^{-2}. At 0000 GMT both the computed and observed values came to 2.93×10^{-4} kg s^{-1} m^{-2}. Since point-by-point agreement was worse at 0000 GMT, it is obvious that the mean rainfall found from a moisture budget analysis gives no indication of the accuracy of individual point values. Perhaps more significantly, the above numbers indicate that, in general, the synoptic scale does provide a sufficient moisture supply to explain the observed rainfall; it is up to the precipitation schemes used and the vertical motion patterns predicted by a particular prognostic model to distribute the amounts accurately. In contrast, Fritsch *et al.* (1976) found that the synoptic scale explained only 20% of the observed rainfall rate measured from a Great Plains squall line. Two possible reasons for this are 1) that within the relatively small area of the squall line, the convection and associated vertical circulations and maximum rainfall rates were more intense than that observed during Agnes, and 2) that the large-scale moisture field was significantly nearer saturation in the Agnes case.

In addition to verifying against observed precipitation data, we have found it useful to construct composite radar, satellite and current weather charts like those shown in Figs. 5 and 6. The symbols used here are the conventional notations used by the National Weather Service facsimile charts except that the cloud top heights are given in hundreds of meters. Here we

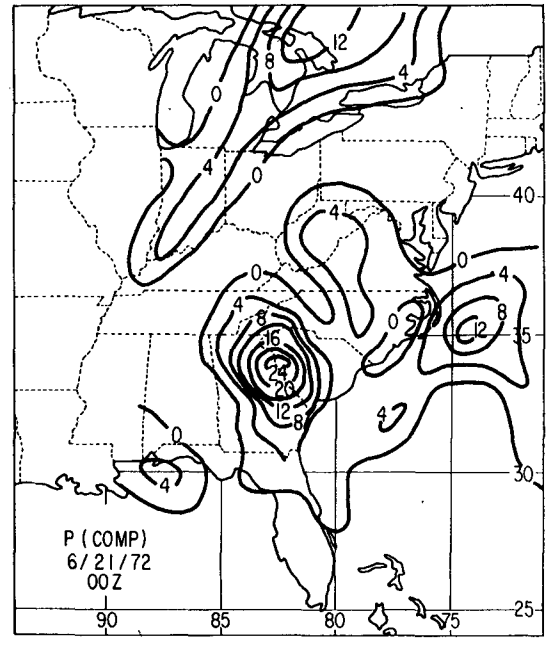

FIG. 4. Computed precipitation rate (10^{-4} kg s^{-1} m^{-2}) from the moisture budget for 0000 GMT 21 June 1972.

can see, for example, the moderate rainfall at 1200 GMT (Fig. 5) in northwest Georgia with tops below 500 mb in agreement with the large-scale induced precipitation indicated in Figs. 1 and 2. At 0000 GMT (Fig. 6) the deep convection associated with the eastern Michigan squall line is clearly indicated. These figures prove most useful, though, when compared to the results computed from stable and convective precipitation schemes, especially over water. Use of these in verifying cloud top heights, type of precipitation, etc., is illustrated in the next section.

To conclude this section, we portray a measure of convective instability to compare with the observed rainfall pattern. Fig. 7 represents the value of

$$\int -\frac{\partial E_s}{\partial p} dp,$$

where $E_s = gz + c_pT + Lq$ is the moist static energy, integrated over all layers where $-\partial E_s/\partial p < 0$ at the 1200 GMT time period. The most prominent feature is the area of low values in the vicinity of the heavy rainfall seen in Fig. 1. Values are somewhat larger in eastern North Carolina and in Michigan where Fig. 5 indicates a more convective regime. The large values over the Gulf of Mexico are due to very dry air overlying the moist boundary layer air; convection is suppressed in this region partially due to subsidence to the rear of Agnes. In general, there is the inverse relationship between convective activity and the degree of convective instability that is usually found in the tropics (see Betts, 1974).

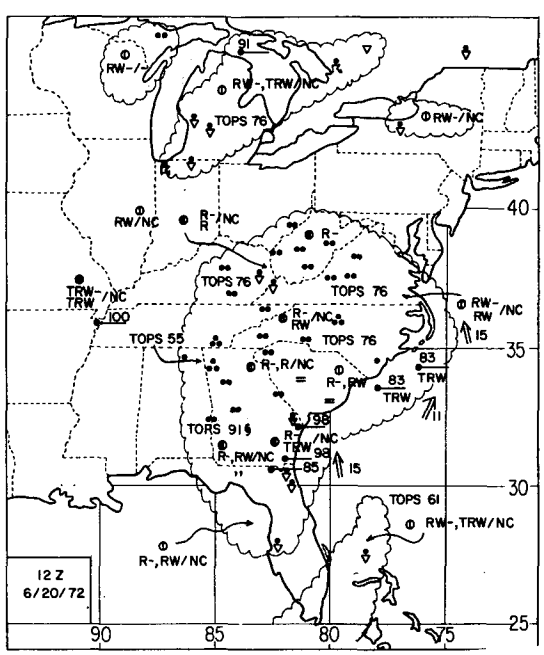

FIG. 5. Composite satellite, radar and current weather chart for 1200 GMT 20 June 1972. Cloud top heights are in hundreds of meters.

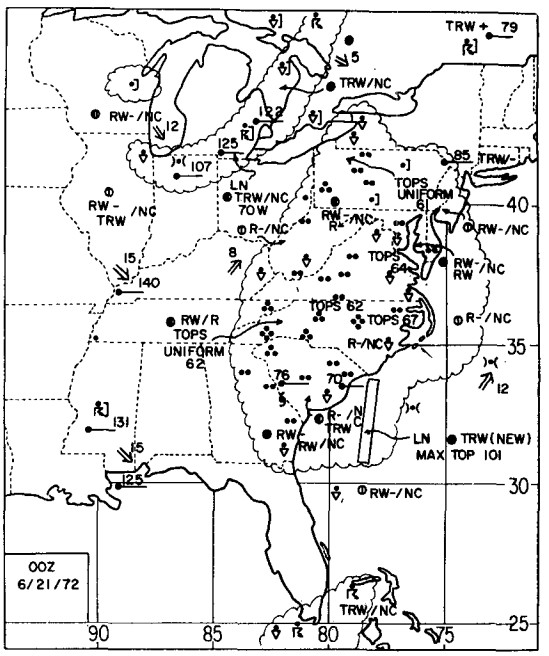

FIG. 6. As in Fig. 5 except for 0000 GMT 21 June 1972.

3. Evaluation and correction of errors in precipitation forecasts

The precipitation predicted by the moisture budget approach does not distinguish between that due to large-scale ascent of stable, saturated air (stable precipitation) and that due to convective processes. In this section, we make further use of the detailed observed rainfall data in an attempt to diagnose the ability of a simple cumulus parameterization scheme to estimate the proper amount of convective precipitation. This will suggest methods that could be used to correct the deficiencies of a particular scheme when it is utilized in a forecast model.

Let the total observed precipitation P_T consist of both stable P_s and convective P_c rainfall at each grid point. The stable or large-scale rainfall can be estimated by several methods (see, e.g., Fulks, 1935; Smagorinsky, 1960; Younkin *et al.*, 1965), most of which are partially derived from the assumption that the rate of precipitation is proportional to the rate of condensation, i.e.,

$$P_s = \frac{1}{g}\int_p \frac{dq_s}{dt} dp.$$

In this study we use the formula for dq_s/dt derived in Haltiner (1971, see p. 163) in which the stable rainfall $\hat{P}_s$ at any one level is given by

$$\hat{P}_s = \frac{\omega q_s T}{p}\left[\frac{LR - c_pR_vT}{c_pR_vT^2 + q_sL^2}\right]. \quad (3)$$

Three criteria need to be satisfied before stable

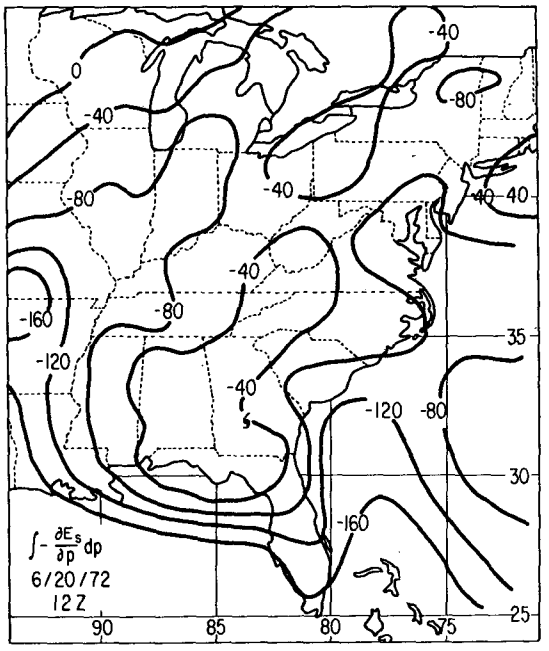

Fig. 7. Sum of $-\partial E_s/\partial p$ ($m^2 s^{-2}$) for all layers where $-\partial E_s/\partial p<0$ for 1200 GMT 20 June 1972.

rainfall is computed:

(i) $\omega<0$, i.e., rising motion is present,
(ii) the relative humidity is $\geq 75\%$,
(iii) the layer must be conditionally stable.

Condition (ii) was chosen from comparison of the analyzed relative humidity fields with the observed precipitation patterns. The last condition was imposed because, in a prognostic model, stable heating is not computed in a conditionally unstable atmosphere in order to prevent gravitational instability on the scale of the grid volume. Recently, Rosenthal and Trout (1977) and Yamasaki (1977), using very fine meshes, have successfully performed numerical simulations of a hurricane without the use of convective parameterization schemes. Although the success of such an approach is obviously grid-size-dependent and more research is needed to examine the physical validity of this procedure, it still might be of some interest to see the difference condition (iii) makes in a diagnostic calculation.

Fig. 8 shows the rainfall rate computed from (3) using 1200 GMT 20 June data when only stable layers are considered. If all layers are used, the rainfall rates are changed to those depicted in Fig. 9. The amount of increase ranges from 50 to 100% at many grid points. Maximum stable heating rates are found just northwest of Agnes and over the southern Appalachians. This is consistent with the observed weather and radar information in Fig. 5. The authors feel that stable and convective rainfall coexist in some sectors of tropical and extratropical storms and that this needs to be considered in numerical models. Mathur (1975), for example, found that nonconvective latent heating at the upper levels in a real-data numerical model of a hurricane was an important factor in the development of realistic hurricane structure.

Radar meteorologists could provide useful information on the existence and relative percentages of stable versus convective precipitation for various magnitudes of conditional instability to help develop a quantitative observational basis for this phenomenon. A determination of the vertical distribution of rainfall and latent heating rates under different synoptic or thermodynamic conditions would also be useful to both modelers and theoreticians.

If we assume that (3) gives an accurate value of P_s, we then have an "observed" value of convective rainfall rate from

$$P_c=P_T-P_s. \tag{4}$$

This value can be compared with that computed from a cumulus parameterization scheme. If we use, for example, the Kuo (1965) formula for convective heating,

$$H_k=\frac{ac_p(T_s-T)}{\Delta\tau},$$

we have the following expression for the convective precipitation rate P_k:

$$P_k=\frac{1}{g}\int_{p_t}^{p_b}\frac{ac_p(T_s-T)}{L\Delta\tau}dp, \tag{5}$$

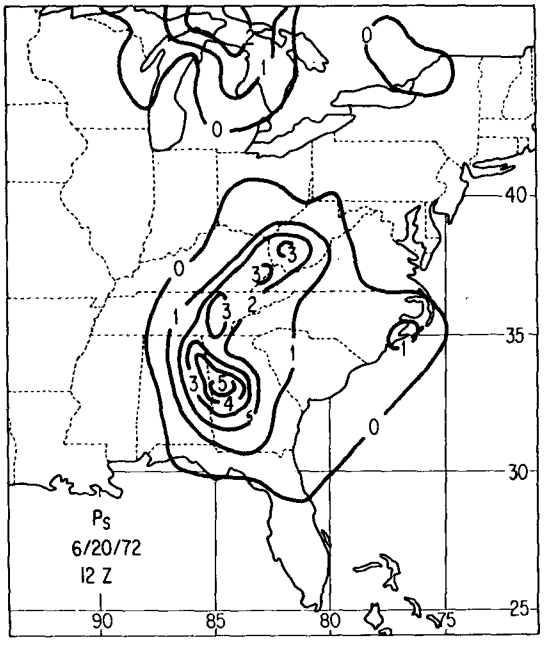

FIG. 8. Stable precipitation rate (10^{-4} kg s^{-1} m^{-2}) computed for 1200 GMT 20 June 1972 when contributions from conditionally unstable layers are not allowed.

where a represents the fractional area of the grid box covered by active convective elements. It is defined by $a=I/Q$ which is the ratio between the actual amount of available moisture to the total amount that the grid volume could contain. See Appendix B for a more complete description of the Kuo scheme applied here.

The value of I is the crucial parameter here, as it represents the upper limit at each point to the amount of convective rainfall that can fall (much of I might actually go into storage, i.e., moistening of the atmosphere). We define I here by

$$I=-\frac{1}{g}\int_{p_t}^{p_b}\frac{\partial wq}{\partial p}dp=-\frac{\omega_b q_b}{g}, \tag{6}$$

where the subscript b refers to cloud base. Hence low-level moisture convergence will determine the intensity of convection.

Since it is unlikely that P_k is everywhere equal to P_c, we will assume that the discrepancy is due to the inexact formulation of the Kuo scheme. Note that the assumption that all of the error is due to the parameterization scheme is not really correct, since much of the error is due to the inaccurately known vertical motion, temperature and moisture fields, quantities whose true values cannot be determined. Since we do know P_T fairly well from detailed hourly data, all of the error will be corrected for by assuming that the parameter I is improperly formulated. Thus we can force the following equality

$$P_c=\lambda P_k=\frac{\lambda I}{gQ}\int_{p_t}^{p_b}\frac{c_p(T_s-T)}{L\Delta\tau}dp \tag{7}$$

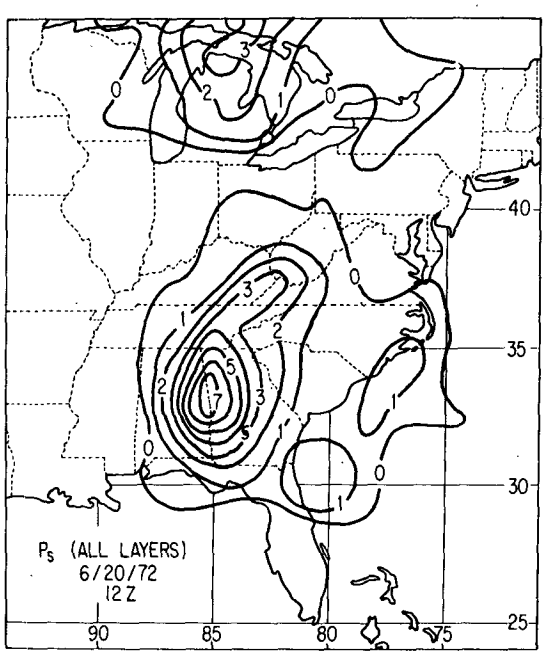

FIG. 9. As in Fig. 8 except that all layers are considered.

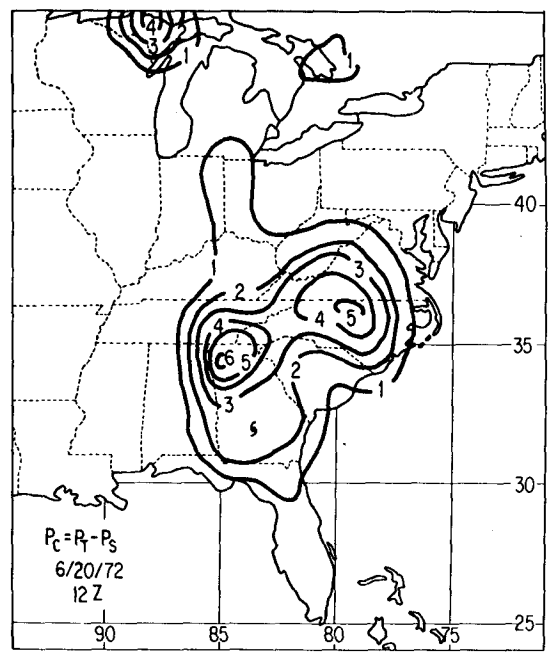

FIG. 10. Convective rainfall rate (10^{-4} kg s^{-1} m^{-2}) needed so that $P_c+P_s=P_T$ at 1200 GMT 20 June 1972.

to hold through the use of the parameter λ. Since λ is the only unknown in (7), we have

$$\lambda=\frac{gL\Delta\tau QP_c}{c_pI\int_{p_t}^{p_b}(T_s-T)dp}. \tag{8}$$

Eq. (8) can also be written

$$\lambda=\frac{P_c}{aQ_1}. \tag{9}$$

In Appendix B we show that aQ_1 represents that part of I that goes into convective precipitation. Thus (9) indicates that λ is a ratio of the amount of convective rainfall that is "observed" to the amount the Kuo scheme actually provides. If $\lambda>1$, it indicates that the value of I was not large enough to allow the Kuo scheme to compute the correct amount of precipitation.

Fig. 10 displays the smoothed values of P_c computed from (4) using 1200 GMT 20 June data. The smoothing operation used here and elsewhere refers to just one pass with the standard nine-point filter. Note that this pattern is not expected to be the exact distribution of observed convective rainfall but that pattern the Kuo scheme, given the fields of ω and P_s that the initial data has yielded, is required to reproduce in order to provide the observed total precipitation at each grid point.

Fig. 11 shows the actual precipitation rate P_k com-

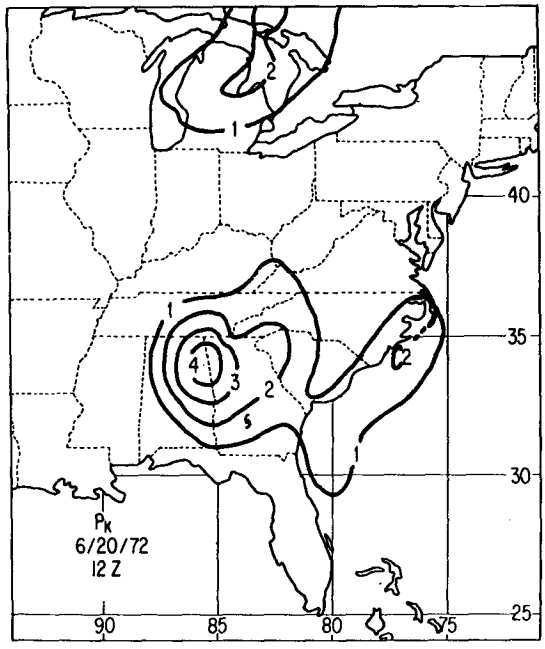

FIG. 11. Convective precipitation rate (10^{-4} kg s^{-1} m^{-2}) computed from the Kuo scheme described in Appendix B for 1200 GMT 20 June 1972.

puted from the Kuo scheme. As expected, it differs significantly from P_c in some areas, especially over North Carolina. Again this is primarily due to the lack of low-level moisture convergence indicated there by the initial data. The maximum P_k is also in northwestern Georgia and northeastern Alabama, where the stable heating was largest, indicating the presence of simultaneous convection and large-scale condensation. The presence of convection in this region is not inconsistent with Fig. 5 since the cloud tops predicted by the Kuo scheme were at 500 mb in this area. The Kuo rainfall also predicts the convection around Lake Huron and off the Carolina coast which is indicated in Fig. 5. Fig. 12 is the "deficiency" map which shows just how much the sum of P_s and P_k fail to yield the observed precipitation rate. Note that in some areas the rainfall rate is slightly overestimated. One encouraging result is the accuracy with which the diagnostic precipitation rate is computed within a 300–400 km radius around Agnes.

In Fig. 13, the deficiency is expressed in terms of λ, i.e., the factor by which the value of I has failed to supply the proper amount of moisture [Eq. (9)]. The hatched area represents those regions where rainfall was observed but λ could not be computed since P_k is zero where $-\partial E_s/\partial p \geqslant 0$ or $I \geqslant 0$. Hence λ goes to infinity in these areas; but, as seen in Fig. 1, this drawback is not too serious due to the light rainfall amounts in the hatched region. This diagram also verifies that the value of I was nearly satisfactory in the area around Agnes. Over eastern North Carolina and westward to Kentucky, we see that two to three times more moisture supply is needed to obtain the observed rainfall.

A useful application of these kinds of calculations is to convert the rainfall deficiency or λ values directly into moisture convergence units. First we define

$$\lambda I_L = I_L + I_M, \tag{10}$$

where I_L represents the usual formula for I given by (6) and I_M is the additional mesoscale or cloud-scale moisture convergence needed to supplement I_L in order to obtain the needed moisture convergence λI_L that yields the observed rainfall. A proper formulation of I_M could be viewed as the primary goal of future parameterization schemes. Diagnostically, a value for I_M is computed from

$$I_M = I_L(\lambda - 1). \tag{11}$$

If $\lambda > 1$, then (11) is positive and I_M is needed to supplement I_L. In those small regions where $\lambda < 1$, then I_L was more than sufficient and will be reduced by I_M. A map of I_M for the 1200 GMT period is presented in Fig. 14. Recall that this pattern not only represents the regions where convective activity was most intense but is also a function of the initial ω field, which in large part determines the patterns of P_s and I_L.

Conceivably, if I_M was derived from the vertical motion field of an initialized state for a prognostic model, a perfect rainfall forecast could be made, at least for the first time step. A new I_M field would be needed at each time step to keep the forecast exact. Unfortunately, with conventional data, I_M can be

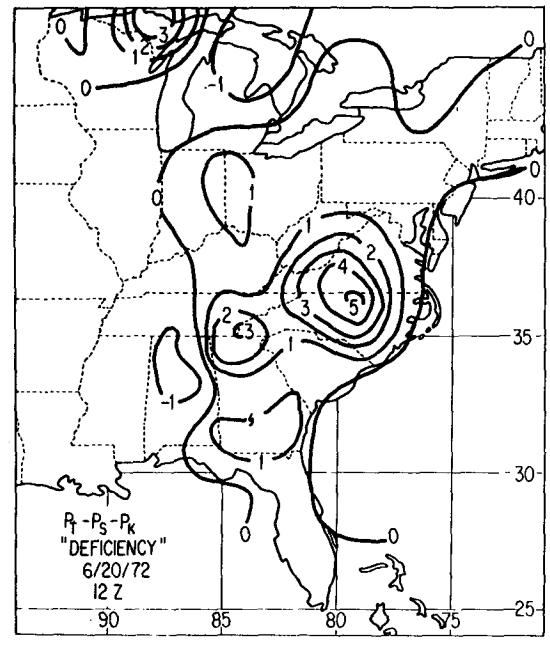

FIG. 12. The difference between the sum of computed stable and convective rainfall rates and the observed rainfall rate (10^{-4} kg s^{-1} m^{-2}) for 1200 GMT 20 June 1972.

computed only every 12 h. Hence an interpolation procedure might be used to produce a time-dependent I_M field. But this second I_M field really isn't valid for correcting the Kuo scheme at $t+12$ h since the ω's given by the observed data are not the same as those that are produced by the forecast. A correct I_M field should be calculated from the observed precipitation and model-derived kinematic and thermodynamic fields. Thus, in a research mode where one might be most interested in simulating the evolution and dynamics of a storm, an interesting but time-consuming iterative procedure could be set up to produce quite accurate forecasts. Starting with the initial I_M field, the forecast would advance 12 h or to any time for which a new P_T field is available (which could be as little as 1 h using hourly rainfall amounts and digitized radar data). A new I_M field could be computed from (11) following the same procedure described in this section. The forecast would then be restarted at the time of the previous I_M, advance to the time of the newest I_M which has increasingly been replacing the old values, and advance through another new P_T time interval whereupon the procedure is repeated.

An alternative method of utilizing the I_M field could be used in a real-time forecasting mode. The original I_M could be applied during the first few hours of the forecast during which it would decrease to zero. Hence, latent heating consistent with the observed rainfall rates would be computed initially and this would lead to the development of motion and thermal fields that are internally consistent with this "observed" heating. In this way, with an initial accurate rainfall forecast, the vertical motion, moisture convergence, etc., fields will adjust toward reality such that the I_M field is not needed after a few hours. Hopefully, realistic patterns will continue to be sustained after I_M vanishes. Care would have to be taken to ensure that mass, heat and moisture budgets were conserved during this procedure.

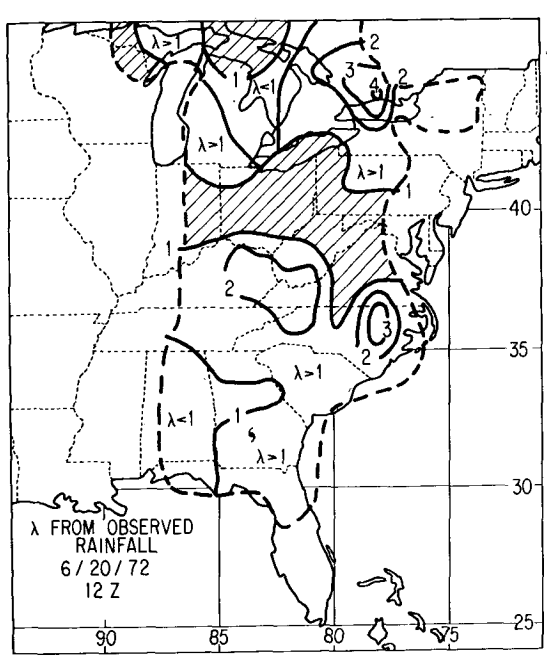

FIG. 13. Factor by which the large-scale moisture supply needs to be increased so that the Kuo scheme yields the P_c field.

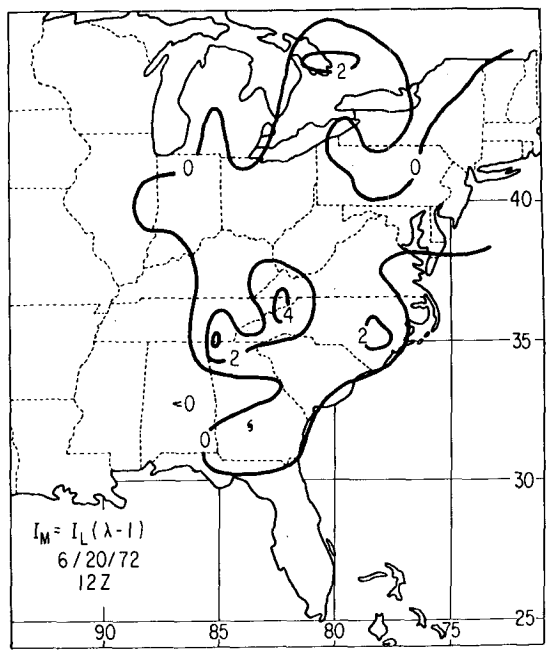

FIG. 14. Subgrid-scale moisture convergence needed for the Kuo scheme to make an accurate convective precipitation forecast for 1200 GMT 20 June 1972.

Of course the most direct way of using observed rainfall data to improve a forecast (in the research mode) is to convert all the P_T fields into latent heating rates such that a time-dependent heating function can be specified at each grid point. Then the forecast could proceed without the need of any stable or convective parameterization schemes and should accurately reproduce the structure, evolution and dynamics of any disturbance in which latent heat is an important energy source. The crucial problem in this approach is to determine the vertical distribution of the specified heating. Two recent approaches to this problem have been taken by Carr (1977) and Molinari (1977, personal communication). It is hoped that all the various approaches described above will be tested during our prognostic studies of Agnes in order to determine the sensitivity of the forecasts to the accuracy of the rainfall predictions.

An independent estimate of λ or I_M can be found from the moisture equation to be used in a prognostic model. For example, let us assume that the following equation is applicable:

$$\frac{\partial q}{\partial t}+\nabla\cdot q\mathbf{V}+\frac{\partial \omega q}{\partial p}=E-\hat{P}_c-\hat{P}_s, \qquad (12)$$

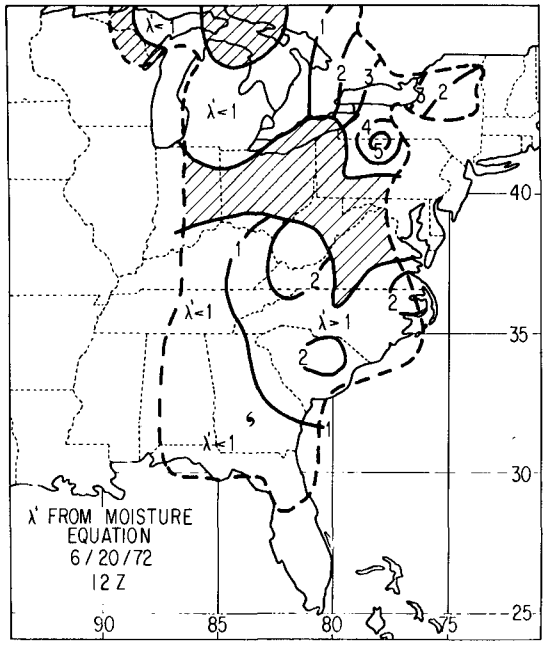

FIG. 15. As in Fig. 13 except that λ′ is derived from the moisture budget equation.

where $\hat{P}_c$ and $\hat{P}_s$ are convective and stable rainfall rates at one level and are computed from (5) and (3) respectively. For the choice of I given by (6), the proper moisture equation becomes

$$\frac{\partial q}{\partial t}=-\nabla\cdot q\mathbf{V}+\frac{a(q_s-q)}{\Delta\tau}+E-\hat{P}_s. \tag{13}$$

If one were to evaluate (13) diagnostically, the left and right sides of the equation would rarely be equal. Again we will assume for convenience that the discrepancy is due to the incomplete formulation of I and force the equality through the use of a λ′ parameter. Integrating with respect to pressure, we have

$$\frac{1}{g}\int_{p_t}^{p_s}\frac{\partial q}{\partial t}dp=-\frac{1}{g}\int_{p_t}^{p_s}\nabla\cdot q\mathbf{V}dp+\frac{\lambda' I}{gQ}\int_{p_t}^{p_b}\frac{q_s-q}{\Delta\tau}dp+E-P_s.$$

Solving for λ′ yields

$$\lambda'=\frac{Q\left[\frac{1}{g}\int_{p_t}^{p_s}\frac{\partial q}{\partial t}dp+\frac{1}{g}\int_{p_t}^{p_s}\nabla\cdot q\mathbf{V}dp-E+P_s\right]}{\frac{I}{g}\int_{p_t}^{p_b}\frac{q_s-q}{\Delta\tau}dp}. \tag{14}$$

Using the definition of a and Q_2 (see Appendix B), we can write (14) as

$$\lambda'=\frac{M}{aQ_2}, \tag{15}$$

where M represents the sum of moisture sources and sinks inside the brackets in (14). Since aQ_2 represents that part of I that goes into moisture storage, λ′ is interpreted as the ratio of the additional moisture sink (or source) needed in the moisture equation to balance the moisture storage (i.e., source) indicated by the Kuo scheme. For example, if $\lambda'>1$, then an additional moisture sink (i.e., more convective rainfall) is needed to balance the moisture equation.

Eq. (15) was evaluated using the same 1200 GMT 20 June data that produced the λ pattern of Fig. 13. Again evaporation is neglected and the tendency term is computed over a 12 h forward difference. The stable and Kuo schemes are computed as before. The resulting λ′ field is shown in Fig. 15. Although some differences exist between Figs. 13 and 15, the area of $\lambda'<1$ west and northwest of Agnes and the regions of $\lambda'>2$ over the Carolinas, central Appalachians and near Lake Ontario are in general agreement. This new λ′ could also be used to compute an I_M field which could be used in the various forecast experiments described earlier. But λ′ is not thought to be as reliable as the first one since (i) the assumption in letting a 12 h q tendency approximate an instantaneous one is poor, (ii) the moisture equation cannot be corrected in regions where no Kuo heating is allowed even though it still might not balance, and (iii) making the q forecast accurate does not guarantee accurate rainfall and latent heating forecasts.

4. Concluding remarks

Quantitative precipitation forecasting remains a critical problem for numerical models and weather forecasters alike. Although statistical methods [particularly MOS, model output statistics (see, e.g., Fawcett, 1977)] and the increasing quantitative use of radar and satellite data promise to improve the situation, dynamical methods still offer the best hope for predicting the *amount* of rainfall, especially for more than 12 h ahead. As seen in Figs. 2, 4 and 12, though, even diagnostic attempts to reproduce an observed rainfall map are not without error. Of course, the discrepancies apparent in Fig. 12 would be smaller if we had made extensive use of cloud physics considerations or had many years of accumulated experience from which to "tune" the precipitation schemes, but the point is that significant errors would still exist, primarily due to errors in the predicted or diagnosed vertical motion fields.

In the preceding section, we showed that if all the error in the rainfall forecast, no matter what it was due to, was attributed to the convective parameterization scheme used, then an expression could be found for the subgrid-scale moisture supply (I_M) that would exactly correct for this error. One of the proposed applications of this I_M field could be used operationally; it would require obtaining the hourly rainfall

reports for the initial time and a few extra minutes of computer time to run one time step of the model, compute the I_M field and then restart the forecast. This experiment as well as the other research mode experiments discussed earlier could provide a unique opportunity, using the Agnes data set, to study the sensitivity of a forecast to the accuracy of the rainfall prediction.

These methods cannot be applied to a model if only convective adjustment accounts for convective precipitation. The Kuo (1965) scheme as modified by Sundqvist (1970) was used here because it is relatively easy and fast to apply, a feature we feel will continue to be required by larger scale models despite the potential improvements in parameterization by more sophisticated, time-consuming schemes. It appears from these results that, if the true vertical motion field were known, the expression for I given by (6) would be adequate. Note that (6) is not the integrated horizontal moisture flux that is applied by some users of Kuo's scheme but is only the vertical moisture flux at cloud base. In addition to being in agreement with CISK theory (Charney and Eliassen, 1964), three reasons for this are: (i) the fact that only air near the boundary layer has sufficiently high E_S values to support deep convection (see Ooyama, 1969), (ii) the favorable situation of low-level convergence beneath strong divergence aloft may not lead to convection in the model if net divergence exists, and (iii) that large-scale middle and upper tropospheric moisture convergence is more likely to be a moisture source for stable precipitation and hence should not be used simultaneously for two purposes.

Fritsch *et al.* (1976), in their study of a Great Plains squall line, found that the use of large-scale moisture convergence would not be appropriate for parameterization of "mid-latitude" convection; rather, that convective rainfall is more a function of preexisting potential buoyant energy. While this is probably a valid conclusion for the central United States and other continental or semi-arid locations in the mid-latitudes (and tropics), it is not as valid for moist synoptic-scale systems that occur in many places around the globe. In many of these systems, convective-scale effects may indeed be diagnosed from large-scale budgets [see, e.g., Cho and Ogura (1974) and Houze and Leary (1976), as well as results from Section 2 and the other moisture budget references], or they may be more accurately deduced from the rate of generation of potential buoyant energy as proposed by Arakawa and Schubert (1974). A specific example where a combination of these effects may be important is the extensive convection in the conditionally unstable regions associated with baroclinic zones in the southeastern United States during winter; in some cases this convection may be an important factor in leading to a subsequent cyclogenetic event (Tracton, 1973). Needless to say, much research is still needed on diagnostic as well as prognostic evaluation of the relative abilities of different parameterization schemes to handle various synoptic and mesoscale situations over different regions of the globe.

Acknowledgments. One of the authors (F.H.C.) would like to thank Professor T. N. Krishnamurti and Dr. M. Kanamitsu for useful discussions on the Kuo scheme. Appreciation is expressed to Andrew Fritz and David Palmiero for assistance in data preparation and to Miss Sally Young for typing the manuscript. This research was supported by the National Science Foundation under Grant A023897-002.

APPENDIX A

List of Symbols

c_p specific heat of air at constant pressure
E evaporation from the earth's surface
E_s moist static energy
g acceleration of gravity
L latent heat of condensation
P precipitation rate
p pressure
q specific humidity
q_s saturated specific humidity
R gas constant for dry air
R_v gas constant for water vapor
T temperature
T_s moist adiabatic temperature
t time
$\mathbf{V}$ horizontal velocity
z geopotential height
ω vertical velocity ($\equiv dp/dt$)

APPENDIX B

The Kuo Parameterization Scheme

The complete convective heating function used in this study is defined by

$$H_c=\alpha H_{c_1}+(1-\alpha)H_{c_2}, \tag{B1}$$

where H_{c_1} is the usual Kuo (1965) heating function

$$H_{c_1}=\frac{ac_p(T_s-T)}{\Delta\tau}. \tag{B2}$$

The cloud time scale $\Delta\tau$ is specified as 30 min, but has no bearing on the size of H_{c_1} since it also appears in the fractional area a, defined by

$$a=\frac{I}{Q}. \tag{B3}$$

Here, the amount of available moisture supply, I is

given by

$$I=-\frac{1}{g}\int_{p_t}^{p_b}\frac{\partial\omega q}{\partial p}dp=-\frac{\omega_b q_b}{g}, \tag{B4}$$

if we assume that $\omega=0$ at cloud top. In (B4), q_b is the specific humidity of cloud base p_b and

$$\omega_b=\tfrac{1}{2}(\omega_{p_b-\Delta p/2}+\omega_{p_b+\Delta p/2}),$$

where $\Delta p=100$ mb.

The total amount of moisture Q needed to heat and moisten the grid volume to the T_s and q_s values of the moist adiabat arising from cloud base is given by

$$Q=Q_1+Q_2=\frac{1}{g}\int_{p_t}^{p_b}\frac{c_p(T_s-T)}{L\Delta\tau}dp+\frac{1}{g}\int_{p_t}^{p_b}\frac{q_s-q}{\Delta\tau}dp. \tag{B5}$$

Note that the moisture supply I can be divided into two parts:

$$I=aQ_1+aQ_2=\frac{a}{g}\int_{p_t}^{p_b}\frac{c_p(T_s-T)}{L\Delta\tau}dp+\frac{a}{g}\int_{p_t}^{p_b}\frac{q_s-q}{\Delta\tau}dp. \tag{B6}$$

The first term on the right side of (B6) represents the amount of the available moisture which falls out as precipitation while the second term is the amount of moisture that remains as water vapor in the atmosphere (moisture storage term).

In order for the Kuo scheme to be applied, the atmosphere needs to be (i) conditionally unstable through at least one layer, defined by $-\partial E_s^*/\partial p<0$, where E_s^*, the saturated moist static energy is given by $E_s^*=c_pT+gz+Lq_s(T)$, and (ii) moisture convergence is positive, i.e., $I>0$.

The need for the second part of the heating function, H_{c_2}, arises whenever the environmental T and q approach T_s and $q_s(T_s)$. Although heavy rainfall can occur under those conditions (e.g., during the mature stage of a hurricane), the H_{c_1} formula isn't suitable since $Q\to 0$ when the moist adiabat is approached. To overcome this deficiency, Sundqvist (1970) used definitions (B2)–(B5) to derive

$$H_{c_2}=\frac{gLI}{p_b-p_t}. \tag{B7}$$

It is also assumed that since q is near $q_s(T_s)$ and $T_s>T$, it has reached $q_s(T)$ (i.e., saturation); thus all of I goes into rainfall at those points and no more storage can occur except as needed to maintain saturation.

The factor α in (B1) allows a smooth transition from H_{c_1} to H_{c_2} as the average $T_s-T(\overline{\Delta T})$ decreases throughout the cloud; it is defined by

$$\alpha=\exp[-(\gamma/\overline{\Delta T})^2],$$

where

$$\overline{\Delta T}=\frac{1}{p_b-p_t}\int_{p_t}^{p_b}(T_s-T)dp$$

and γ is an arbitrary constant equal to 0.70. Note that when the H_{c_2} is being used (whenever $\overline{\Delta T}<3$°C), the formula actually used for the λ derived in Section 3 [Eq. (9)] is

$$\lambda=\frac{P_c}{I(1-\alpha)+\alpha aQ_1}. \tag{B8}$$

When $\alpha=1$, $H_c=H_{c_1}$ and (B8) reduces to (9). If $\alpha\to 0$, then $\lambda=P_c/I$, which indicates that all of I is going into rainfall. In this study, we found that the use of this Sundqvist correction increased the convective rainfall up to a factor of 3 at some grid points.

REFERENCES

Arakawa, A., and W. H. Schubert, 1974: Interaction of a cumulus cloud emsemble with the large-scale environment. Part I. *J. Atmos. Sci.*, **31**, 674–701.

Benton, G. S., and M. A. Estoque, 1954: Water-vapor transfer over the North American continent. *J. Meteor.*, **11**, 462–477.

Betts, A. K., 1974: Thermodynamic classification of tropical convective soundings. *Mon. Wea. Rev.*, **102**, 760–764.

Bosart, L. F., and F. H. Carr, 1978: A case study of excessive rainfall centered around Wellsville, New York, 20–21 June 1972. *Mon. Wea. Rev.*, **106**, 360–374.

Bradbury, D. L., 1957: Moisture analysis and water budget in three different types of storms. *J. Meteor.*, **14**, 559–565.

Carr, F. H., 1977: Numerical simulation of a mid-tropospheric cyclone. FSU Rep. No. 77-1, Dept. of Meteor., Florida State University, 267 pp.

Charney, J. G., and A. Eliassen, 1964: On the growth of the hurricane depression. *J. Atmos. Sci.*, **21**, 68–75.

Cho, H.-R., and Y. Ogura, 1974: A relationship between cloud activity and the low-level convergence as observed in Reed-Recker's composite easterly waves. *J. Atmos. Sci.*, **31**, 2058–2065.

Danard, M., 1968: Water balance of extratropical cyclones. *Atmosphere*, **6**, 129–132, 149–150.

Fankhauser, J. C., 1965: A comparison of kinematically computed precipitation with observed convective rainfall. Tech. Note 4-NSSL-25, National Severe Storms Laboratory, 28 pp.

Fawcett, E. B., 1977: Current capabilities in prediction at the National Weather Service's National Meteorological Center. *Bull. Amer. Meteor. Soc.*, **58**, 143–149.

Fernandez-Partagas, J. J., and M. A. Estoque, 1974: An observational study of convergence and rainfall over South Florida. *J. Appl. Meteor.*, **13**, 507–509.

Fritsch, J. M., C. F. Chappell, and L. R. Hoxit, 1976: The use of large-scale budgets for convective parameterization. *Mon. Wea. Rev.*, **104**, 1408–1418.

Fulks, J. R., 1935: Rate of precipitation from adiabatically ascending air. *Mon. Wea. Rev.*, **63**, 291–294.

Haltiner, G. J., 1971: *Numerical Weather Prediction*. Wiley, 317 pp.

Houze, R. A., Jr., and C. A. Leary, 1976: Comparison of convective mass and heat transports in tropical easterly waves computed by two methods. *J. Atmos. Sci.*, **33**, 424–429.

Hudson, H. R., 1971: On the relationship between horizontal

moisture convergence and convective cloud formation. *J. Appl. Meteor.*, **10**, 755–762.

Kuo, H. L., 1965: On formation and intensification of tropical cyclones through latent heat release by cumulus convection. *J. Atmos. Sci.*, **22**, 40–63.

Mathur, M. B., 1975: Development of banded structure in a numerically simulated hurricane. *J. Atmos. Sci.*, **32**, 512–522.

O'Brien, J. J., 1970: Alternative solutions to the classical vertical velocity problem. *J. Appl. Meteor.*, **9**, 197–203.

Ooyama, K., 1969: Numerical simulation of the life cycle of tropical cyclones. *J. Atmos. Sci.*, **26**, 3–40.

Rosenthal, S., and J. W. Trout, 1977: A propagating squall system observed in the pre-hurricane phase of an axisymmetric tropical cyclone simulation. Presented at AMS Conf. on Numerical Weather Prediction, Omaha.

Smagorinsky, J., 1960: On the dynamical prediction of large-scale condensation by numerical methods. *Physics of Precipitation, Geophys. Monogr.*, No. 5, Amer. Geophys. Union, 71–78.

Spar, J., 1953: A suggested technique for quantitative precipitation forecasting. *Mon. Wea. Rev.*, **81**, 217–221.

Starr, V. P., and R. M. White, 1955: Direct measurement of the hemispheric poleward flux of water vapor. *J. Mar. Res.*, **14**, 217–225.

Sundqvist, H., 1970: Numerical simulation of the development of tropical cyclones with a ten-level model. Part I. *Tellus*, **22**, 359–390.

Tracton, M. S., 1973: The role of cumulus convection in the development of extratropical cyclones. *Mon. Wea. Rev.*, **101**, 573–593.

Yamasaki, M., 1977: A preliminary experiment of the tropical cyclone without parameterizing the effects of cumulus convection. *J. Meteor. Soc. Japan*, **55**, 11–30.

Younkin, R. J., J. A. LaRue and F. Sanders, 1965: The objective prediction of clouds and precipitation using vertically integrated moisture and adiabatic vertical motions. *J. Appl. Meteor.*, **4**, 3–17.